ChemPubSoc Europe

DOI: 10.1002/open.201800076

Open Access ChemistryOPEN Communications

VIP

The Reduction of Dissolved Oxygen During Magnesium Corrosion

Eduardo L. Silva,*[a] Sviatlana V. Lamaka,[a] Di Mei,[a] and Mikhail L. Zheludkevich[a, b]

The consumption of dissolved oxygen (DO) during the corrosion of commercially pure magnesium specimens was investigated by localized corrosion techniques. The concentration of oxygen and the local current density on the near-surface of magnesium were measured simultaneously by a micro-optode DO sensor and the scanning vibrating electrode technique (SVET), respectively. Diamond microelectrodes were also used for DO mapping. Significant DO depletion was found since the initial immersion time of Mg in NaCl 0.5 M, and a correlation could be established between DO consumption and areas of anodic and cathodic activity. These findings assume particular relevance for the corrosion of Mg alloys or magnesium components with impurity levels higher than the tolerance limit. Moreover, this study points out the significance of the partial oxygen pressure as an influential parameter during magnesium corrosion.

Understanding and controlling the corrosion of magnesium and magnesium alloys has been the focus of many professionals of the academic and industrial sectors in recent years. Such endeavors are aimed at increasing the use of these materials in structural applications such as the aerospace, automotive or biotech industries, mostly because of the low density of Mg and its high strength-to-weight ratio.[1] The corrosion behavior of magnesium-based materials is one of the characteristics that makes them unique. This is because corrosion can either be one of the main drawbacks of magnesium structures (for example in the automotive industry) or its core working principle, which is the case for biodegradable magnesium implants.[1] Thus, before magnesium can find its way into a wider span of applications and be established as a key structural material, a unified corrosion theory and reproducibility of measurements among research groups is essential.[2,3] Some examples of this lack of consistency include the clarification of enhanced hydrogen evolution during anodic polarization and the disparity observed between in vitro and in vivo measurements during the biological-induced degradation of Mg alloys.[2,4–6] Contrary to most corrosion scenarios observed in other metals, during the corrosion of magnesium, dissolved oxygen (DO) is widely disregarded as an important cathodic reagent.[6–9] Undoubtfully, there is compelling evidence that water reduction is the main cathodic reaction during magnesium corrosion, with abundant hydrogen evolution.[6,10,11] However, in recent years, there is increasing evidence showing that the oxygen reduction reaction (ORR) might have a higher significance than commonly expected. Wang and co-workers have demonstrated that a significant difference in potentiodynamic behavior can be found for the magnesium alloy AZ31 under aerated and deaerated conditions in various NaCl concentrations.[12] The authors have attributed the higher current density observed in aerated conditions to the oxygen reduction reaction. In a recent work from Snihirova and colleagues, the DO concentration was found to be depleted on the near-surface of magnesium coupled to aluminum and copper.[13] This is quite an unexpected behavior considering that copper should present the highest cathodic activity in this type of system. Recently, new models focusing on the explanation of the enhanced hydrogen evolution observed during anodic polarization on magnesium provide further support for the role of dissolved oxygen on the corrosion of Mg. Höche and co-workers indicated re-deposition of iron and other heavy metal impurities as the principal mechanism underlying the abnormal hydrogen evolution observed during anodic polarization of magnesium.[14] Later, Marcus et al. found additional experimental evidence for Fe re-deposition.[15] A similar mechanism was proposed by Li and co-workers who demonstrated a copper re-deposition occurring during the corrosion of AZ91.[16] Upon non-Faradaic release from the Mg matrix, copper is no longer cathodically protected by magnesium and undergoes oxidation, with the ORR as the main cathodic reaction.

In this work, localized corrosion techniques were used to study the oxygen gradients that can develop during the corrosion of magnesium and their phenomenological correlation with the local corrosion activity. Two different types of oxygen sensors were used for comparison, the first based on DO sensing by optochemical oxygen quenching,[17] as described in Ref. [18] and the second consisting of electrochemical reduction of DO on the surface of a carbon-based microelectrode.[19] Figure 1 shows DO line measurements obtained for a commercially pure magnesium specimen immersed in NaCl 0.5 M, with an oxygen sensitive micro-optode. The data were recorded simultaneously with local current density measurements by SVET. A visible oxygen depletion can be observed when the

[a] Dr. E. L. Silva, Dr. S. V. Lamaka, D. Mei, Prof. Dr. M. L. Zheludkevich
MagIC—Helmholtz-Zentrum Geesthacht
Max-Planck-Straße 1, 21502 Geesthacht (Germany)
E-mail: eduardo.trindade@hzg.de

[b] Prof. Dr. M. L. Zheludkevich
Institute for Materials Science, Kiel University
Kaiser Str. 2, 24143 Kiel (Germany)

Supporting Information and the ORCID identification number(s) for the author(s) of this article can be found under: https://doi.org/10.1002/open.201800076.

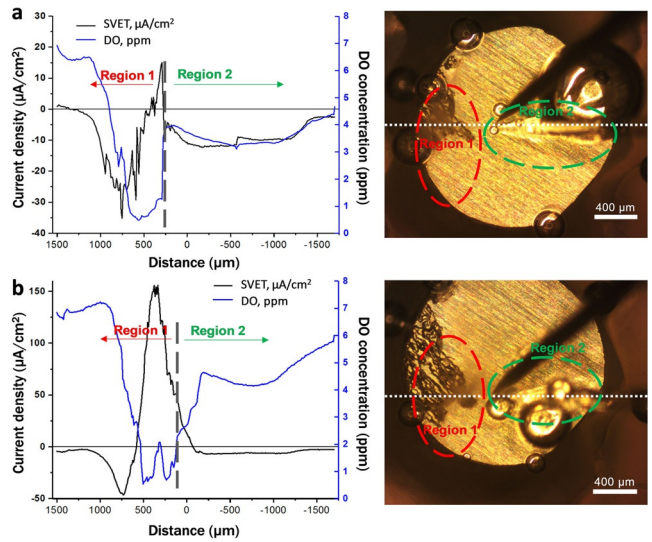

Figure 1. Simultaneous SVET and DO linear measurements across the Mg surface in air saturated 0.5 M NaCl flowing through the cell at a rate of 0.5 mL min^{-1}. DO depletion in the a) net cathodic region taken 11 min since the beginning of immersion and b) DO depletion over an active anodic and slow cathodic region of the specimen, taken 17 min since the beginning of immersion.

DO sensor is scanning over magnesium. Figure 1 shows the development of two types of regions: Region 1, which is characterized by actively developing dark areas of corrosion products and intense H_2 evolution; and Region 2, which is a visually passive area with no visible corrosion products. The local current densities as measured by SVET indicate that despite the visible corrosion of magnesium in Region 1, this area can exhibit net cathodic activity as shown in Figure 1 a, with a minor anodic spike at the corrosion front. In the subsequent measurements, there is a clear development of the anodic activity until it eventually dominates Region 1, i.e., the rate of oxidation of Mg^0 to Mg^{II} becomes much higher than the rate of cathodic activity (Figure 1 b). In Region 2, the measured current density shows that cathodic processes are always more significant, although at times an equilibrium condition is almost reached (Figure 1 b). In both regions the DO level typically reaches very low values of <1 ppm (Figure 1 a). Such intense depletion is comparable to the minimum DO concentration registered for copper connected to aluminum and magnesium in Ref. [13]. DO mapping with the micro-optode combined with current density measurements (Figure 2) provided a broader insight of the developing oxygen gradients. Both sensors were positioned at distance of 100 ± 5 μm from the specimen's surface at the beginning of the measurements in the X–Y plane. The map took 50 min to acquire and the active front of filiform corrosion progressed quickly during this time. By overlapping the SVET and DO maps (Figure 2 d), the lowest DO concentration can be assigned to the area mediating Regions 1 and 2. This shows that DO consumption can be assigned to the ORR occurring in areas of cathodic predominance and anodic predominance as well. Although water reduction [Eq. (1)] is kinetically favored over ORR [Eq. (2)] on magnesium, the latter reaction can occur on both the Mg matrix as well as

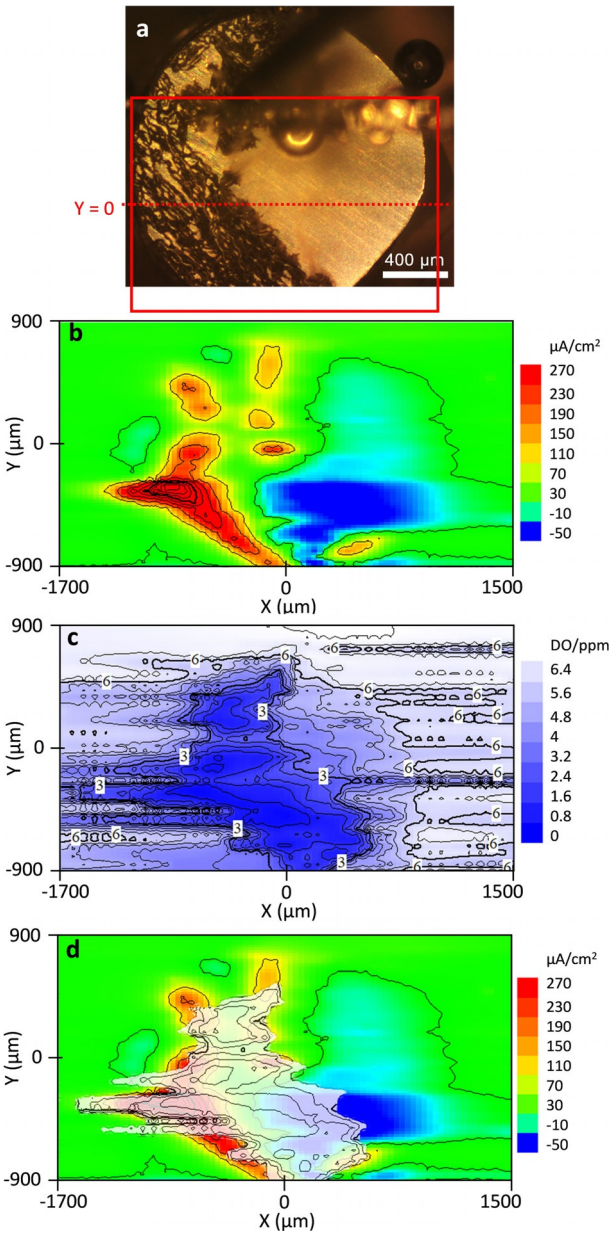

Figure 2. SVET and DO mapping of commercially pure Mg. The local current densities of the specimen (a) are shown in (b) where anodic and cathodic activity are occurring at coordinates $Y<0$. The DO concentration recorded with the micro-optode is shown in (c) and overlapping of both maps can be seen in (d) showing that DO depletion is occurring over the most active region of the specimen.

on other microstructurally distinct regions such as intermetallic phases and impurity particles rich in transition metals (such as Fe, Ni or Cu). According to recent evidence, these particles can be electrically disconnected from the bulk material during the corrosion of magnesium.[14,20] When transition-metal-rich particles are detached from Mg, they can undergo self-corrosion. In this case, as long as the corrosion potential of the particles is more positive than the standard potential for water reduction (-0.83 V_{SHE}), the ORR can become the predominant cathodic reaction supporting the oxidation of the impurity metals. Upon re-deposition on the surface of magnesium, impurities

create conditions for enhanced HER, which perpetuates the impurity deposition cycle until the entire magnesium specimen is converted to corrosion products.[14] The possibility of hydrodynamic effects caused by hydrogen evolution were considered in the present work, namely how H_2 bubbles might influence the concentration of DO in Region 2, leading to local displacement of the dissolved gas.

$$2\,H_2O + 2\,e^- \rightarrow H_2 + 2\,OH^- \quad (1)$$

$$O_2 + 2\,H_2O + 4\,e^- \rightarrow 4\,OH^- \quad (2)$$

Figure 3 shows DO mapping with boron-doped diamond microelectrodes (BDD). The main advantage of these microsensors in comparison to the micro-optode is the speed of data acquisition, which can be twice as fast. Thus, they were used for the acquisition of DO sequential maps, between 0–25 min (Figure 3 a) and between 50–75 min of immersion time in NaCl 0.5 M (Figure 3 b). In these measurements the BDD microelectrode is polarized at −1 V vs. Ag|AgCl to promote DO reduction on its surface. Thus, less negative current values correspond to areas where there is higher DO depletion. Similar to previous observations for the SVET/micro-optode maps, oxygen depletion can be observed in both Region 1-type areas (Figure 3 a) and Region 2-type areas (Figure 3 b). In this case, however, these regions are spatially very distinct. Figure 3 b shows that DO depletion can be intense over Region 2 while being negligible over Region 1, even though strong H_2 evolution was occurring when the sensor was scanning over Region 1. This observation supports the idea that DO consumption is indeed a result of the ORR rather than DO displacement as a result of hydrodynamic effects arising from H_2 evolution. (A DO increase on the near-surface of some stationary big H_2 bubbles was also detected. This current increase is most likely related to the temporary adsorption of big H_2 bubbles on the microelectrode surface as it scans by, which causes a disturbance in the local electric field as well as enhanced mass transport due to non-uniform shear forces exerted by the bubble.[21,22])

Further clarification of the effect of H_2 evolution on the local concentration of DO was gathered by measuring DO concentration in a setup where the source of hydrogen was separated from the effects of the magnesium surface (Figure 4 a). In this setup, H_2 was generated in a small container with 0.5 g of pure Mg chips immersed in NaCl 0.5 M (surface area ≈48 $cm^2\,g^{-1}$) at a rate of approximately 20 $cm^3\,h^{-1}$. The hydrogen gas was conducted to a cell where the micro-optode was scanning across an aperture of ≈170 μm diameter, from which H_2 bubbles were being released (Figure 4 b and Video 1 in the Supporting Information). During the first minutes, no significant DO depletion was observed, i.e., the DO concentration line was very identical to the reference line when no H_2 was bubbling (Figure 4 c). After 15 mins of H_2 purging, the DO concentration slightly diminished from around 7 ppm to a minimum of 6.15 ppm. For an identical immersion time, the DO concentration above the corroding Mg specimen in Figure 1 a, b is lower than 1 ppm. The concentration continued to decrease not just

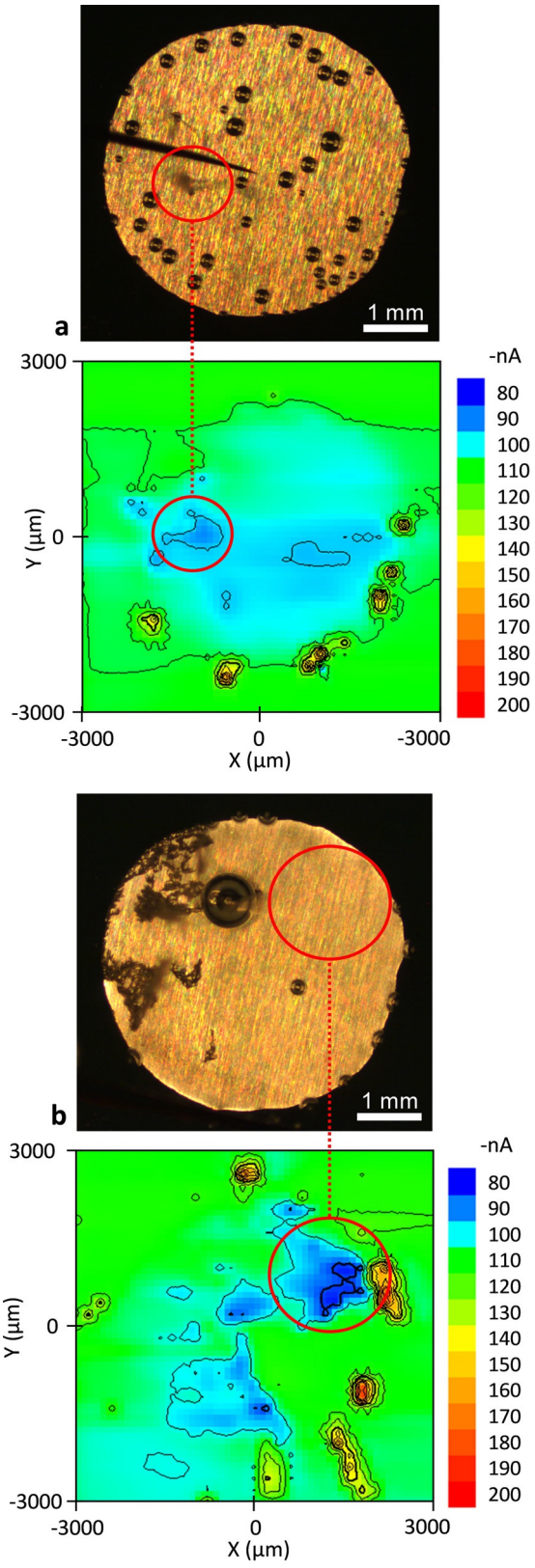

Figure 3. DO reduction current maps recorded with the diamond microelectrode. Less negative current corresponds to lower dissolved oxygen concentration. a) DO depletion between 0 and 25 immersion minutes can be observed mainly over a corrosion pit. b) For a 50–75 min immersion time, the DO concentration is lowest over a corrosion-free area, most likely as a result of ORR on impurity-rich particles imbedded in the barrier layer.

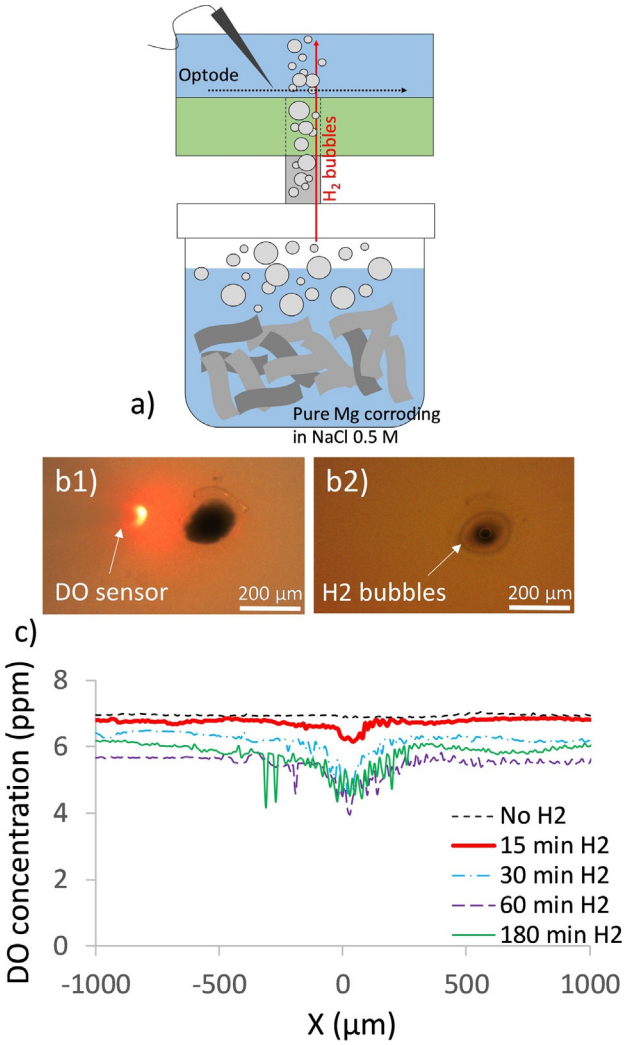

Figure 4. DO measurements on a cell with hydrogen bubbling through a hole with ≈170 µm diameter (b1, b2), after being generated in a separate container with 0.5 g of pure magnesium immersed in NaCl 0.5 M, as depicted in (a). The real setup during the experiment can be visualized in Video 1 in the Supporting Information. DO depletion increases with time until it reaches a minimum around 4 ppm for 1 h purging time. This minimum concentration did further decrease until up to 3 hours at least, as shown in (c).

above the orifice but also around it, as can be seen by the downshift in the baseline for extended purging times (Figure 4c). After 1 h of hydrogen purging, a minimum DO concentration of approximately 4 ppm was reached. For longer purging time, up to 3 h at least, this remained the minimum concentration that could result from DO being purged by H_2 (Figure 4c). Moreover, it is important to notice that the surface area of the Mg specimen in Figure 1 is ≈0.03 cm^2, that is, about 800 times less than the surface area of the Mg chips in the H_2 generation container in Figure 4. Thus, the DO concentration profiles shown in Figure 4c demonstrate that under the corrosion conditions investigated in this work, H_2 evolution alone cannot be responsible for the depletion of DO to concentrations below 1 ppm, as shown in Figure 1. The depletion of DO on the surface of magnesium is, therefore, related to oxygen reduction on the surface of the metal.

Impurities are always present in magnesium and there is growing evidence that the corrosion of magnesium is strongly influenced by the oxidation and re-deposition of not only impurities like Fe, but also of other elements used for Mg alloying.[15,23] This context suggests that dissolved oxygen is a very important cathodic reagent during the corrosion of magnesium. Furthermore, considering that the partial oxygen pressure in human physiological conditions is 30 mmHg,[24] about five times lower than in normally aerated conditions, our study indicates that, accounting for DO alone, the corrosion rate of metallic implants in vivo should be lower than in simulated fluids or in vitro conditions. Although this tendency has indeed been confirmed by several authors, some of the given reasons include the difficulty in mimicking in vivo conditions.[4] Thus, a future work will address the influence of oxygen during the corrosion of Mg alloys in physiological simulated environments.

Summarizing, this work presents strong evidence pointing to dissolved oxygen as more than a by-standing species during the degradation of Mg, with pronounced depletion in both anodically and cathodically activated areas, as shown by SVET and localized DO measurements. These results are in alignment with modern theory of magnesium corrosion and provide further support to the active role of impurity-rich particles during magnesium corrosion.

Experimental Section

Specimen Preparation and DO Sensors

Commercially pure magnesium (99.8%, Goodfellow, Fe 45 ppm, Ni 12 ppm, Cu 16 ppm) rods were imbedded in epoxy resin to create a model cell with suitable dimensions for mounting in a commercial SVET (scanning vibrating electrode technique) system (Applicable Electronics Inc., USA). Before mounting, the specimen was ground with 4000 grit sandpaper with high purity ethanol to avoid corrosion, and ultrasonically cleaned in ethanol afterwards.

For dissolved oxygen detection, a commercial sensor was used (FireStingO2 fiber-optic oxygen micro-sensor from Pyroscience™). The fiber-optic microsensor and its application to corrosion studies are described elsewhere.[18] Independently, a second DO microelectrode, based on boron-doped diamond, was used. The preparation of these probes was carried out by chemical vapor deposition, with subsequent surface modification by CF_4 plasma in order to provide sensitivity to DO, according to Ref. [19]. For SVET, insulated Pt–Ir probes (Microprobe, Inc.) with platinum black deposited to form a spherical tip of 15 µm diameter was used as vibrating electrode.

A "hydrogen generator" was prepared by immersing 0.5 g of commercial purity magnesium (Fe 342 ppm) in NaCl 0.5 M in a small plastic container (Figure 4a). This container was connected to a cell consisting of an epoxy resin cylinder with an orifice through which H_2 was released into NaCl 0.5 M and finally to the atmosphere, as described in Figure 4a and Video 1 in the Supporting Information. The NaCl solution was made to flow through the cell at a flow rate of 0.5 mL min^{-1} by using a peristaltic pump. This setup was used to investigate the purging effect of H_2 evolution on DO. The hydrogen evolution rate of this "generator" was measured separately by using eudiometers (art. nr. 2591-10-500 from Neubert-

Glas, Germany). The measurements were conducted by immersing 0.5 g of Mg chips (surface area $\approx 48\ cm^2 g^{-1}$) in NaCl 0.5 M for 5 h (see Figure S1 in the Supporting Information).

Electrochemical Measurements

The corrosion behavior of the model Mg specimen was studied by SVET using a commercial apparatus from Applicable Electronics, controlled by the ASET/LV4 software (Sciencewares). The probe was vibrating in the planes perpendicular (Z) and parallel (X) to the sample's surface. The amplitude of vibration was 32 μm (peak-to-peak), the vibration frequencies of the probe were 124 Hz (Z) and 325 Hz (X). SVET measurements were performed simultaneously with measuring DO by the micro-optode. The distance between SVET and DO probes during dual scanning was 90 μm in the Y plane.

The monitoring of the dissolved oxygen content was also performed using the oxygen-sensitive diamond microelectrode, polarized at −1 V vs. Ag|AgCl applied by an IPA2 amplifier in a two-electrode arrangement, with an Ag/AgCl minielectrode as counter and reference electrode. During the measurements, all the sensors were positioned at 100 ± 5 μm above the sample surface and were moved stepwise across the surface by using a microstepping motor driver (USDIGITAL, USA). By using a peristaltic pump, the electrolyte solution was flowing constantly at a flow rate of $\approx 0.5\ mL\ min^{-1}$ to ensure a constant supply of oxygen.

Acknowledgements

E.L.S. would like to acknowledge the European Commission for the Marie Skłodowska-Curie Individual Fellowship (IF-EF), Grant Agreement 703566—MAGPLANT, conceded in the frame of the H2020-MSCA-IF-2015 programme. D.M. thanks the China Scholarship Council for the award of fellowship and funding (No. 201607040051).

Conflict of Interest

The authors declare no conflict of interest.

Keywords: corrosion · dissolved oxygen · localized measurements · magnesium · oxygen reduction reaction

[1] J. F. King, *Mater. Sci. Technol.* **2007**, *23*, 1 – 14.
[2] M. P. Staiger, F. Feyerabend, R. Willumeit, C. S. Sfeir, Y. F. Zheng, S. Virtanen, W. D. Müeller, A. Atrens, M. Peuster, P. N. Kumta, D. Mantovani, F. Witte, *Mater. Sci. Eng. B Solid-State Mater. Adv. Technol.* **2011**, *176*, 1596 – 1599.
[3] E. Willbold, A. Weizbauer, A. Loos, J. M. Seitz, N. Angrisani, H. Windhagen, J. Reifenrath, *J. Biomed. Mater. Res. Part A* **2017**, *105*, 329 – 347.
[4] A. H. M. Sanchez, B. J. C. Luthringer, F. Feyerabend, R. Willumeit, *Acta Biomater.* **2015**, *13*, 16 – 31.
[5] A. Myrissa, N. A. Agha, Y. Lu, E. Martinelli, J. Eichler, G. Szakács, C. Kleinhans, R. Willumeit-Römer, U. Schäfer, A. M. Weinberg, *Mater. Sci. Eng. C* **2016**, *61*, 865 – 874.
[6] M. Esmaily, J. E. Svensson, S. Fajardo, N. Birbilis, G. S. Frankel, S. Virtanen, R. Arrabal, S. Thomas, L. G. Johansson, *Prog. Mater. Sci.* **2017**, *89*, 92 – 193.
[7] G. L. Makar, *J. Electrochem. Soc.* **1990**, *137*, 414 – 421.
[8] G. Baril, N. Pébère, *Corros. Sci.* **2001**, *43*, 471 – 484.
[9] T. Beldjoudi, C. Fiaud, L. Robbiola, *Corrosion* **1993**, *49*, 738 – 745.
[10] M. Gobara, M. Shamekh, R. Akid, *J. Magnes. Alloy.* **2015**, *3*, 112 – 120.
[11] R. W. Revie, H. H. Uhlig, *Corrosion and Corrosion Control: An Introduction to Corrosion Science and Engineering, 4th ed.*, John Wiley & Sons, Inc., New Jersey, **2008**.
[12] L. Wang, T. Shinohara, B.-P. Zhang, *Mater. Trans.* **2009**, *50*, 2563 – 2569.
[13] D. Snihirova, M. Taryba, S. V. Lamaka, M. F. Montemor, *Corros. Sci.* **2016**, *112*, 408 – 417.
[14] D. Höche, C. Blawert, S. V. Lamaka, N. Scharnagl, C. Mendis, M. L. Zheludkevich, *Phys. Chem. Chem. Phys.* **2016**, *18*, 1279 – 1291.
[15] D. Mercier, J. Światowska, S. Zanna, A. Seyeux, P. Marcus, *J. Electrochem. Soc.* **2018**, *165*, C42 – C49.
[16] J. Li, W. Sun, B. Hurley, A. A. Luo, R. G. Buchheit, *Corros. Sci.* **2016**, *112*, 760 – 764.
[17] H. N. McMurray, P. Douglas, C. Busa, M. S. Garley, *J. Photochem. Photobiol. A* **1994**, *80*, 283 – 288.
[18] M. G. Taryba, M. F. Montemor, S. V. Lamaka, *Electroanalysis* **2015**, *27*, 2725 – 2730.
[19] E. Silva, A. C. Bastos, M. Neto, A. J. Fernandes, R. Silva, M. G. S. Ferreira, M. Zheludkevich, F. Oliveira, *Sens. Actuator B Chem.* **2014**, *204*, 544 – 551.
[20] M. Taheri, J. R. Kish, N. Birbilis, M. Danaie, E. A. McNally, J. R. McDermid, *Electrochim. Acta* **2014**, *116*, 396 – 403.
[21] H. Liu, L. Pan, J. Wen, *Can. J. Chem. Eng.* **2016**, *94*, 192 – 199.
[22] J. Dukovic, C. H. Tobias, *J. Electrochem. Soc.* **1987**, *134*, 331 – 343.
[23] E. Michailidou, H. N. McMurray, G. Williams, *ECS Trans.* **2017**, *75*, 141 – 148.
[24] M. Morita, T. Sasada, I. Nomura, Y. Q. Wei, Y. Tsukamoto, *Ann. Biomed. Eng.* **1992**, *20*, 505 – 516.

Received: May 2, 2018

